Synsint Research Group

Available online at www.synsint.com

Synthesis and Sintering

ISSN 2564-0186 (Print), **ISSN** 2564-0194 (Online)

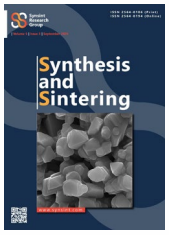

Research article

Effects of sintering and pressing conditions on the properties of manganese ferrite

Aida Faeghinia

Ceramics Department, Materials and Energy Research Center (MERC), P.O. Box 31779-83634, Karaj, Iran

ABSTRACT

In the present work, zinc-manganese ferrite powder with stoichiometric composition Fe_2O_3-0.5ZnO-0.5Mn_3O_4 was prepared by mixing the constituent oxides and sintering them. The samples were shaped by two methods: dry powder pressing and slurry pressing with 10% water by weight (after drying), with a pressure of 50 MPa. The samples were sintered in a tube furnace in different oxidizing, neutral, and reducing atmospheres at 1050 °C. Under a neutral argon atmosphere, the porosity was reduced by about 2%, compared to the sintering samples in the oxide state. In order to achieve zero porosity, pressing using a slurry is more effective in small-sized parts. Samples sintered in nitrogen atmosphere, at the same temperature and sintering conditions, had smaller grain sizes compared to those sintered in hydrogen and oxide atmospheres. Based on microstructure comparison, sintering in a hydrogen atmosphere probably led to the formation of the gamma phase in ferrite. The change in magnetic permeability of the samples made by slurry and pressing methods was not significant; with increasing frequency, the permeability increased by about 20% in both cases.

© 2025 The Authors. Published by Synsint Research Group.

KEYWORDS

Ferrite
Pressing
Sintering
Furnace atmosphere

OPEN ACCESS

1. Introduction

Soft ferrites are a class of ceramic-based soft magnetic materials that combine high electrical resistivity with low magnetic losses, making them ideal as cores for transformers, inductors, and other electromagnetic components operating from hundreds of kilohertz up to several gigahertz [1]. Among the various types of soft ferrites, manganese–zinc (Mn–Zn), nickel–zinc (Ni–Zn), and lithium–titanium (Li–Ti) ferrites are the most widely used. Because the processing techniques are broadly similar, research on Mn–Zn ferrites provides valuable insights for other compositions as well [2]. In contrast, hard ferrites such as strontium or barium ferrite exhibit high coercivity and relatively permanent magnetization, whereas soft ferrites have low coercivity, so their magnetization can reverse with little energy and minimal heat generation, a key requirement for high-frequency power electronics [3].

Soft ferrites are typically produced from iron-oxide powders reacted in the solid state with divalent or trivalent metal oxides such as zinc, manganese, nickel, cobalt, or magnesium to tailor the desired properties [4]. Achieving a high degree of chemical homogeneity at the powder-mixing stage is critical because it governs phase formation, grain growth, and consequently the magnetic and electrical behavior of the final component. Conventional processing involves powder mixing, granulation, drying, calcination (typically 800–1100 °C), milling to sub-micron sizes, spray drying and shaping, followed by high-temperature sintering (generally 1200–1400 °C) to densify the compact [5].

Among the various process parameters, the sintering atmosphere has been shown to exert a profound effect on the phase assemblage, grain size, and magnetic performance of ferrites. Reducing atmospheres such as hydrogen or carbon monoxide can partially reduce Fe^{3+} to Fe^{2+} and Mn^{3+} to Mn^{2+}, altering the Fe^{2+}/Fe^{3+} ratio and magnetic permeability,

* Corresponding author. *E-mail address:* a.faeghinia@merc.ac.ir (A. Faeghinia)

Received 3 November 2024; Received in revised form 26 September 2025; Accepted 26 September 2025.

Peer review under responsibility of Synsint Research Group. This is an open access article under the CC BY license (https://creativecommons.org/licenses/by/4.0/).

https://doi.org/10.53063/synsint.2025.53260

but excessive reduction may generate unwanted phases and lower the electrical resistivity of soft ferrites [5, 6]. Conversely, oxidizing atmospheres (air or pure oxygen) stabilize higher oxidation states, suppress secondary phases, and improve insulation resistance [7]. Inert atmospheres such as argon or nitrogen are employed when preservation of the initial stoichiometry is critical, for example, to limit zinc volatilization or to prevent excessive oxidation [8]. Recent work on Ni–Cu–Zn ferrites has confirmed that even small variations in oxygen partial pressure during sintering can markedly change the crystal structure and magnetic enhancement [9]. Similar findings have been reported for Mn–Zn ferrites, where controlling the partial oxygen pressure reduces power loss and preserves composition during high-frequency operation [10].

The forming method is another key determinant of microstructure and properties. In the dry-pressing route, ferrite powders are compacted under high pressure and then sintered; this is suited to mass production of simple shapes with good green density, but the uniformity of microstructure depends strongly on powder quality and compaction conditions [11]. Wet or slurry pressing introduces a liquid carrier (typically water) to improve particle rearrangement and reduce magnetic orientation effects during pressing, which can lower porosity in small parts [12]. Extrusion and injection-molding techniques allow fabrication of complex shapes with finer dimensional control, but they also require strict management of binder burnout, sintering temperature, and furnace atmosphere to avoid secondary phases or defects [13]. Recent studies on Mn–Zn ferrites have demonstrated that combining optimized pressing with controlled atmospheres yields higher densities, reduced porosity, and improved permeability compared with conventional practice [14].

Taken together, these studies highlight that the simultaneous optimization of furnace atmosphere and forming method is essential for producing Mn–Zn and related ferrites with the desired magnetic and electrical characteristics. In this work, we investigate the role of sintering atmosphere (oxidizing, inert, and reducing) and the effect of two forming methods (dry pressing and slurry pressing) on the density, shrinkage, and microstructure of composite ferrites. Understanding these interactions provides a pathway to manufacture small ferrite components with lower porosity, improved uniformity, and stable high-frequency performance.

2. Experimental procedure

For each batch, commercial and industrial grade 8.27 g of Mn_3O_4, 8.14 g of ZnO, and 31.94 g of Fe_2O_3 were weighed and thoroughly mixed with ethanol using one large and one small milling ball to ensure complete dispersion of the oxides. The mixed powders were calcined at 700–900 °C to initiate the solid-state reactions and subsequently milled to reduce the particle size to below 1 µm. After milling, 1–10 wt% polyvinyl alcohol (PVA) and 10 wt% carboxymethyl cellulose (CMC) were added as a binder, and the powder was hand-mixed in a plastic bag to achieve a uniform binder distribution. The resulting mixture was pressed into 2 cm diameter compacts under a pressure of 211 g cm^{-2}, with approximately 2 g of powder fed into the mold and compacted three times to obtain uniform green bodies. Sintering was performed at 950–1050 °C with a heating rate of 10 °C min^{-1} for 2 h under controlled atmospheres of argon, hydrogen, or nitrogen.

Porosity, water absorption, and density were measured according to ASTM C373-88: samples were dried at 100 °C, cooled in a desiccator, weighed, and then immersed in water for 24 h to determine the saturated weight. X-ray diffraction (XRD) analysis was used to identify the crystalline phases in the glass-ceramic samples. In this analysis, a Philips PW 3710 device with Cu Kα radiation at a wavelength of 1.54 Å, under a voltage of 40 kV and a current intensity of 30 mA in the range of 2θ = 5–80 ° was used. The identification of phases present in the sample powders was done using X'Pert High Score software.

In order to investigate the microstructure of the heat-treated samples, they were first polished with polishing paper ranging from 400 to 2500, then chemically etched in 3% HF solution for 1 minute, rinsed with distilled water, dried, coated, and examined using a field emission scanning electron microscope (MIRA3 TESCAN). The real and imaginary parts of the complex magnetic permeability were determined on an Agilent E4991A RF impedance/material analyzer in the 10^7–10^9 Hz frequency range, using an Agilent 16454A magnetic material test fixture.

3. Results and discussion

3.1. Effects of sintering conditions on density

The conditions of the sintered samples under different conditions and the properties obtained are summarized in Table 1. First, the samples were sintered in an oxide atmosphere in a box furnace at a heating rate of 10 °C/min to a temperature of 980–1050 °C, and then, given that the porosity of these samples was between 8 and 10 wt%, sintering was carried out under a neutral atmosphere. It is observed that the samples with low binder content (samples 6 and 7) tend to delaminate, and even if they appear to be in good condition, they show cracks after sintering in the furnace. It has been said that while the orientation of the ferrite crystals is beneficial in many ways, it causes certain problems in the manufacture of magnets. When the raw ferrite is formed into a magnet, it is found that shrinkage in different directions within the magnet is significant. For example, in an anisotropic strontium ferrite magnet, the shrinkage is about 31% in each direction. On the other hand, the hot magnet maintains the shrinkage at only about 18% in all directions [7]. It is understood that in an anisotropic magnet, any misalignment of the crystals in any part of the magnet affects the magnitude of the shrinkage in the orientation parallel and perpendicular to the direction of the magnet. Cracking during sintering has an effect. Even if the magnets do not crack, warping and distortion often occur during sintering, requiring expensive grinding operations to smooth the surfaces of the magnets. This undesirable ferrite crystal misalignment may be caused by various phenomena, including the fringes of the magnetic field of the die, the turbulence of the powder as it is pressed, and the friction of the die [8], since the walls of the die have friction in relation to the compaction of the blank, thus having a fringe effect. As a result, the magnetic lines of force for the powder moving during pressing are directed at the edges of the curved magnetic field, although they may be perfectly straight in the center of the magnetic field. Accordingly, the material at the pressed edge of the blank will have crystals aligned with the curved lines of magnetic force, and therefore these crystals will not be pressed and aligned parallel to the crystals in the center (samples 1 to 3) [9]. The turbulence effect is a consequence of the movement of the slurry during pressing because the velocity of the water flow may tilt the particles or move them out of alignment with the magnetic lines of force.

Table 1. Properties of the sintered samples under different conditions.

Sample No.	Shaping method	Holding time, h	Paste	Appearance	Atmosphere	Porosity, %	Shrinkage, %	Density, g/cm^3
1	Dry press	2	CMC	Matt	Oxidizing	4.5	18	3.71
2	Dry press	2	CMC	Cracked	Oxidizing	9	18	3.39
3	Dry press	2	CMC	Flaking	Oxidizing	10	18	
4	Dry press	2	4 wt% PVA	-	Argon	2	19.5	4.88
5	Dry press	2	4 wt% PVA	-	Argon	2.5	18.95	4.36
6	Dry press	2	1 wt% PVA	Tendency to delaminate	Oxidizing	1.81	16.5	4.14
7	Dry press	2	4 wt% PVA	-	Oxidizing	1	15.5	4.12
8	Slurry	2	10% humidity	-	Argon	1	18	4.7
9	Slurry	2	10% humidity	-	Argon	2.9	19.8	4.25
10	Slurry	Slow heating rate	10% humidity	Two phases with different color	Oxidizing	1.8	17.1	3.10
11	Slurry	High heating rate	10% humidity	-	Argon		16.2	-
12	Slurry	2 h	10% humidity	-	Oxidizing	1	15.5	4.1
13	Slurry	High heating rate-1 h	10% humidity	Two phases with different color	N_2-argon	6	21.7	3.39
14	Slurry	Slow heating rate-1 h	10% humidity	Two phases with different color	H_2-argon	5.7	20	3.9
15	Dry powder	Muffle	10 wt% PVA	-	Oxidizing	7.9		4.62
16	Dry powder	Slow heating rate -1 h	10 wt% PVA	-	H_2	1	22	4.22
17	Slurry	Slow-1 h	H_2	-	H_2	7	18	4.1
18	Calcinated	1 h	Oxide	-	Oxidizing	7	15	4.22

The effect of die wall friction is quite logical because, as the die wall moves in contact with the pressed blank, crystal particles may move out of alignment with the magnetic lines of force [9]. These various effects are particularly significant where the magnets produced are relatively small in size. That is, where the smallest cross-sectional dimension of the magnet, perpendicular to the orientation direction, is less than five times the thickness of the blank magnet in a direction parallel to the orientation direction of the crystals [7]. On the other hand, during the thermal re-sintering (calcination) process, very fine powders with particle sizes less than 0.1 µm also grow simultaneously in the ceramic slurry, which improves the residual water removal capacity during the subsequent forming process and thus enhances the magnetic properties. Since thermal re-sintering is used for ground powder with an average particle size (D50) of approximately 0.55 µm, it can be ensured that the powder grains grow to a certain extent during the thermal annealing process, thereby achieving a high proportion of grains in a magnetic domain [10]. Thus, according to Table 1, the full density of 5.33 g/cm^3 expected for the ferrite piece was not achieved, although the density increased from 3.37 g/cm^3 to 4.33 g/cm^3 in the final ferrite piece by changing the furnace atmosphere from an oxidizing atmosphere.

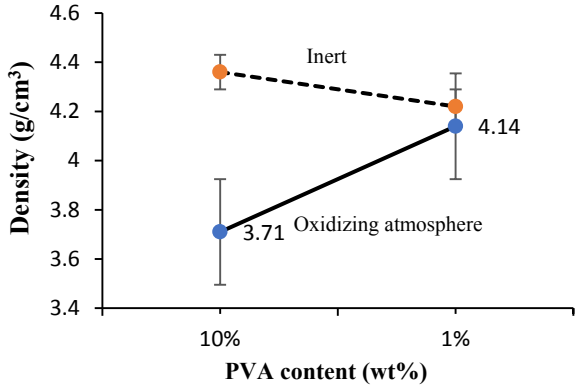

Fig. 1. Density changes in terms of adhesive percentage for two furnace atmospheres.

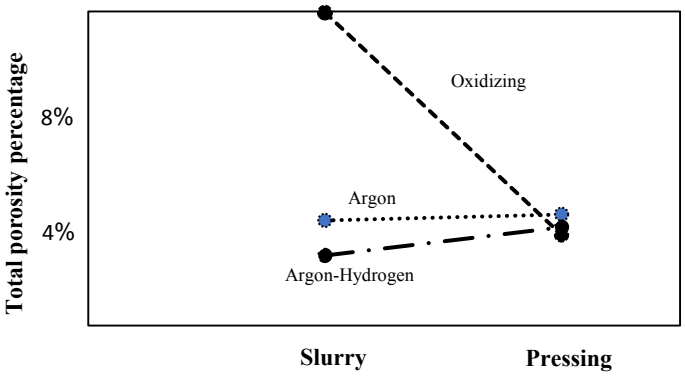

Fig. 2. Porosity changes in terms of part forming method in three sintering furnace atmospheres (samples 11,14, 9, 6).

3.2. Effects of adhesive and furnace atmosphere on density

The graph of density changes after sintering of sintered parts in an oxidizing and neutral atmosphere in terms of PVA percentage is shown in Fig. 1. Heating was performed at a temperature of 400 °C to remove the adhesive. According to the figure, with increasing the amount of adhesive due to increased porosity in the oxide atmosphere, the density decreases, but in the case of samples sintered in neutral conditions, this is the opposite, and the increase in adhesive probably causes greater adhesion and higher density, and the adhesive remains in the environment as carbon. In some cases, it may be desirable to completely sinter the ferrite plate before cutting, in which case a temperature of about 1050 °C is used [11].

3.3. Effects of the forming method on density

While ferrite powder may be pressed in dry conditions, the use of a slurry is generally more satisfactory to prevent magnetic orientation of the powder in contact with the mold. Preferably, the main fluid ingredient of such a slurry is water. Therefore, as shown in Fig. 2, the forming conditions were changed from dry powder pressing to slurry mud pressing, and the results of the porosity changes in these two forming methods are presented in terms of sintering atmosphere with a sintering temperature of 1050 °C.

As can be seen, the porosity of the ferrite samples decreases with the change in the controlled atmosphere from argon to argon-hydrogen. The use of an argon-hydrogen atmosphere in the ferrite sintering process reduces porosity compared to sintering under oxidizing atmospheres, which is probably due to the reduction of oxidation, since in an argon-hydrogen atmosphere, the metal compounds of the materials in the ferrite are less likely to be oxidized, since hydrogen plays a reducing role [12]. As a result, the formation of Fe_3O_4 oxides, which may cause the formation of inhomogeneous and porous phases in the oxidized atmosphere, is reduced. Hydrogen in this atmosphere can react with some impurities and oxides, such as nickel as impurities and remove them from the structure, which helps to improve the wettability between ferrite particles [13]. This improvement in

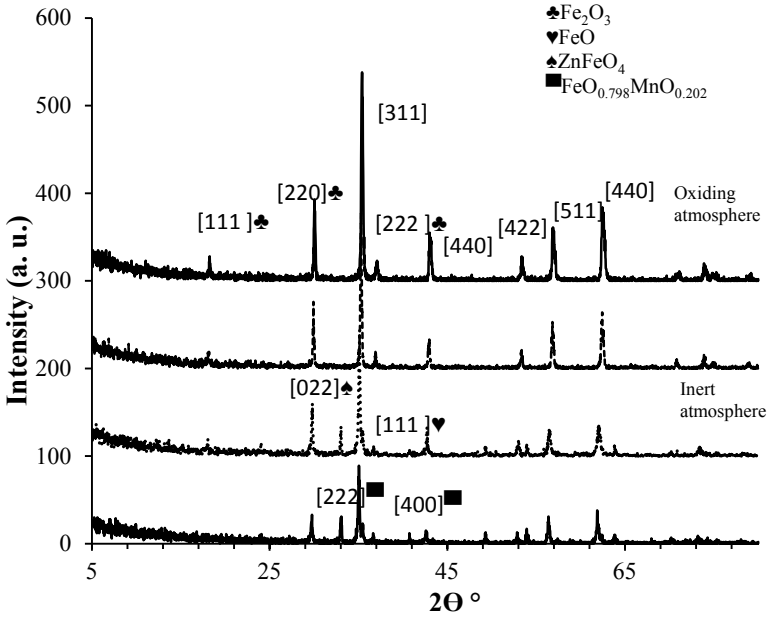

Fig. 3. XRD patterns of the sintered samples.

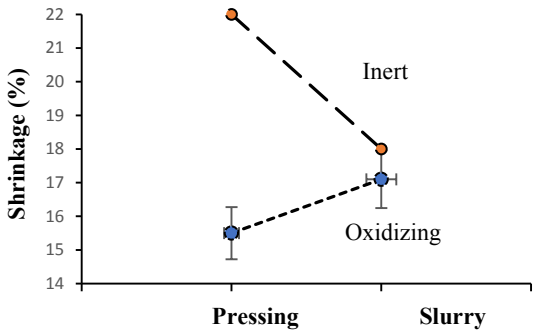

Fig. 4. Changes in shrinkage according to production method for two furnace atmospheres (samples 4, 7, and 9).

wettability increases the density and reduces the void space (porosity) in the final material. In the oxidized condition, Fe_2O_3 and ZnO react together, and the divalent zinc ion reacts with the trivalent iron ion in the spinel structure to form the zinc ferrite structure $ZnFe_2O_4$, as shown in Fig. 3 by the X-ray diffraction results.

In the presence of argon-hydrogen, such reactions are minimized, but a more homogeneous structure is formed, which reduces porosity. On the other hand, in a reducing atmosphere, the wetting of iron oxide FeO with zinc and manganese oxides is much greater than the wetting of these oxides with Fe_2O_3 [14]. Therefore, since the FeO structure is more stable in the reducing atmosphere, the adhesion to Mn_2O_3 materials is greater, as shown in the X-ray diffraction pattern in Fig. 3. But this can be detrimental to the magnetic properties of the magnet. For this purpose, XRD analysis was performed.

3.4. Phase evaluation

It should be noted that the X-ray diffraction patterns of different iron oxide phases, such as magnetite and hematite, overlap; therefore, distinguishing between these phases requires complementary analyses. Here, since the magnetic properties are of greater importance than the crystalline phases, X-ray diffraction was performed only for general phase identification, as shown in Fig. 3.

In spinel ferrites, under oxidizing atmospheres, the reaction between Fe_2O_3, ZnO, and MnO leads to the formation of spinel ferrites. Spinel ferrites generally have the formula $(Zn, Mn)Fe_2O_4$. This phase can include zinc ferrites ($ZnFe_2O_4$) and manganese ferrites ($MnFe_2O_4$), which form composite phases through partial or total substitution of Zn and Mn in the spinel structure [15]. However, in neutral atmospheres, similar spinel-type phases such as $(Zn, Mn)Fe_2O_4$ still form, but due to the reduced effects of strong oxidation, the formation of reduced phases such as MnO may also be possible. MnO and ZnO may remain partially in neutral atmospheres or react with Fe_2O_3 to a lesser extent, because the complete oxidation of cations to Fe^{+3} may be limited due to the lack of sufficient oxygen. If the sintering process is carried out at high temperatures and for a long time, there is a possibility of the formation of composite spinel phases similar to the ferrites formed in an oxide atmosphere, but the formation of some intermediate oxides, such as Fe_3O_4 (magnetite), is also possible [16].

In a reducing atmosphere, some phases such as MnO may also remain. That is, Mn_2O_3 (manganese III oxide) can be reduced to MnO (manganese II oxide) in a hydrogen atmosphere at high temperatures. Mn_2O_3 is stable in an oxidizing environment, but in a neutral or reducing atmosphere such as argon, it tends to lose oxygen and be reduced to Mn_3O_4 (hausmannite) and finally to MnO with increasing temperature. The general reactions can be expressed as follows:

$$Mn_2O_3 \rightarrow Mn_3O_4 \text{ at moderate temperatures} \quad (1)$$

$$Mn_3O_4 \rightarrow MnO \text{ at higher temperatures} \quad (2)$$

The final reduction to MnO occurs at temperatures usually above 900–1000 °C in an argon atmosphere. This reduction is common in processes where manganese oxides are exposed to non-oxidizing or reducing conditions during high-temperature heat treatment [17]. To

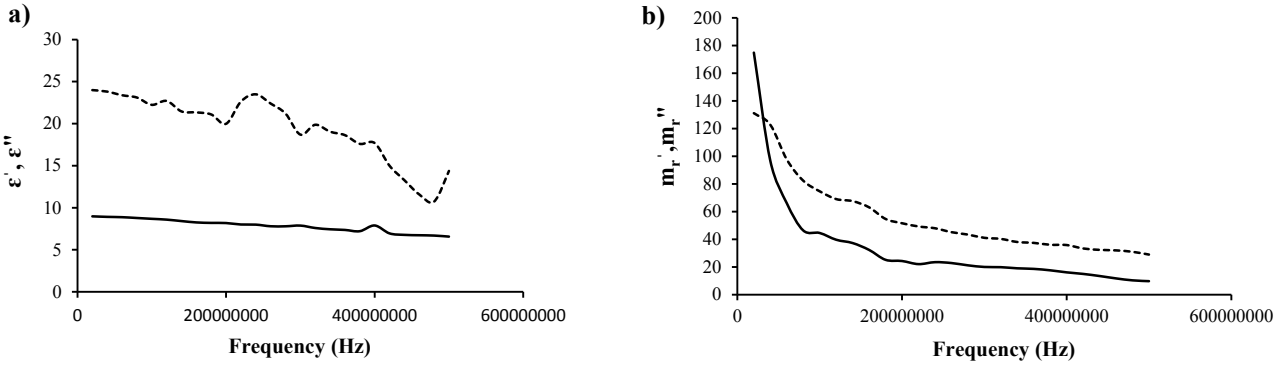

Fig. 5. Virtual and real parts of a) electric and b) magnetic permittivity vs. frequency in double-sintered oxide samples.

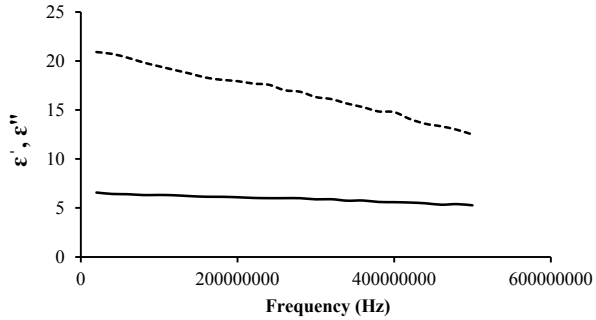

Fig. 6. Virtual and real parts of electric permittivity vs. frequency in slurry sintered samples.

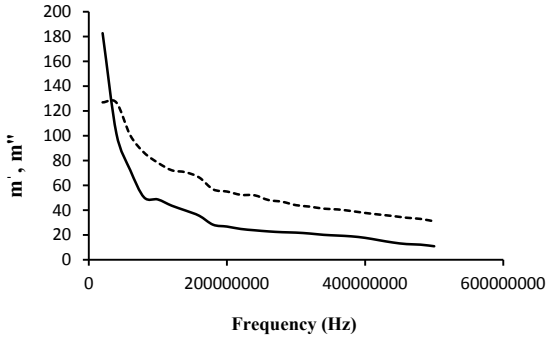

Fig. 7. Virtual and real parts of magnetic permeability vs. frequency in slurry sintered samples.

further investigate this issue, shrinkage and microstructural examination were performed on the samples.

3.5. Shrinkage of the samples sintered under different atmospheres

Since accurate shrinkage calculation is required for mold design, two different forming methods with two different atmospheres were compared in terms of shrinkage, and the results are presented in Fig. 4.
A notable point in sintering with the neutral method is that in the tube furnace, due to the temperature limitation, samples 8 to 13 were sintered up to 950 °C. The slow heating rates and the holding time at the sintering temperature also increased. Two-phase samples with different fixtures and colors were observed (probably due to the excessive growth of crystals in the sample). The porosity of these samples increased, so they were not used for further investigation. The sintered, powdered, and re-sintered samples, although having less shrinkage, still had a porosity of less than 10% [18]. In general, the reasons for the different shrinkage in the samples can be attributed to abnormal grain growth. Abnormal grain growth or cracking during sintering of spinel ferrites can be caused by several factors related to microstructural evolution. The exact causes may be due to local variations in particle size, porosity (slurry samples with high water content), or temperature at different rates at which they densify. The heating rate of slurry samples is much lower than that of dry samples. This uneven densification can cause internal stress and lead to cracking or warping of the material. If the temperature distribution during sintering is not uniform, parts of the sample may sinter faster than others, causing differential shrinkage and consequently cracking. If the raw materials (e.g., Fe_2O_3, ZnO, and MnO) are not mixed uniformly at the molecular level, some regions may have different stoichiometry, leading to abnormal grain growth or different sintering rates. This can create weak spots or stress concentrations that lead to cracking. The release of volatile compounds or gases (such as residual carbon or trapped gases from PVA adhesives) during sintering can lead to increased stress in certain regions, causing cracks or abnormal grain growth. This is the case for slurry samples sintered in oxidized conditions, which leads to increased shrinkage [18]. In multicomponent spinel ferrites, different phases may have different thermal expansion coefficients. During heating or cooling, these inhomogeneities can create internal stresses, especially at grain boundaries, leading to cracking. Spinel ferrites are sensitive to oxygen levels during sintering. Insufficient oxygen supply can lead to the formation of oxygen vacancies that destabilize the structure, while excessive oxygen may cause unwanted oxidation of some elements, leading to grain growth anomalies. If the green body is not uniformly densified (due to the magnetic effect of the mold and matrix), the resulting density variations can lead to different sintering behavior, with some regions shrinking more than others, causing cracking or warping [19].
These various effects are particularly noticeable where the hardened

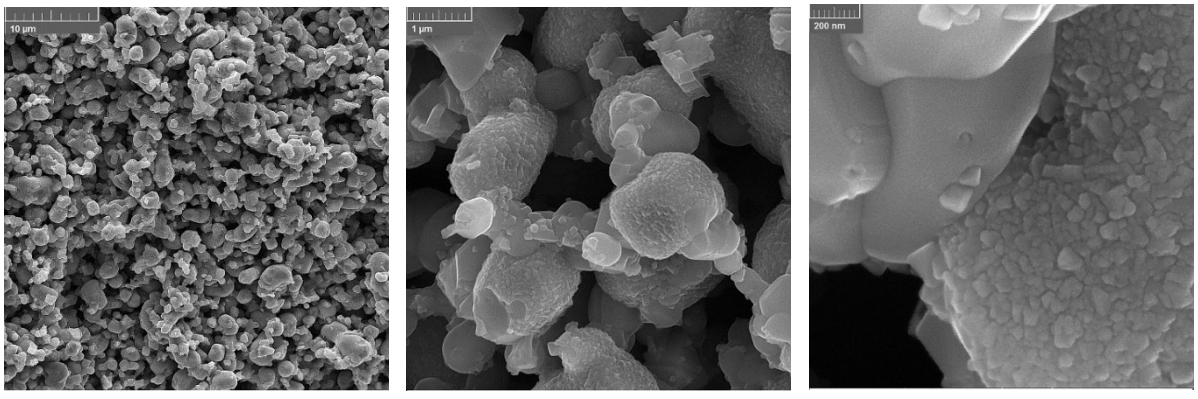

Fig. 8. SEM images of sample 12 sintered and pressed under oxidizing atmosphere.

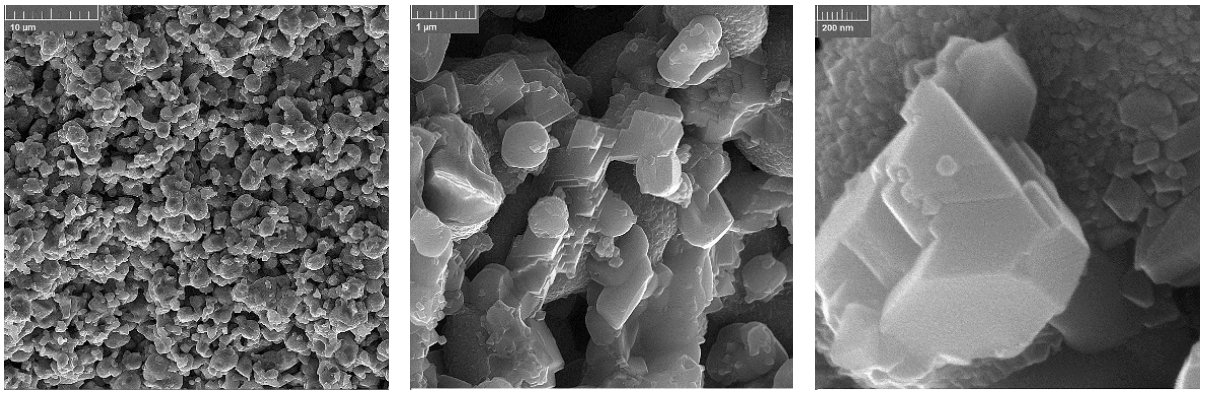

Fig. 9. SEM images of sample 13 sintered and pressed under a nitrogen atmosphere.

steels produced are relatively small in size, meaning that in places where the smallest dimension of the magnetic cross-section perpendicular to the orientation direction is less than five times the thickness of the raw hardened steel in a direction parallel to the crystal orientation [18]. On the other hand, in the process of secondary heat re-sintering, very fine powders with particle sizes less than 1.0 micrometers will also grow simultaneously in the ceramic dough, improving the removal capacity of the remaining water in the subsequent shaping process and thus improving the magnetic properties. From the point of view that secondary heat re-sintering is used for milled powders with an average particle size of about 1.00 micrometers, it can be ensured that the powder particles grow to a certain extent in the subsequent annealing process, and also a relatively high proportion of particles in a specific area.

3.6. Magnetic properties

Usually, an increase in the percentage of shrinkage means a higher density of particles in the material. Increased compaction usually improves contact between particles and reduces porosity, which can lead to an increase in magnetic permeability (μ). This is due to a decrease in the magnetic resistance of the paths within the material. In the case of the slurry sample, the shrinkage is greater than that of the oxide sample, resulting in a permeability of about 4% higher than that of the oxide sample, but in the case of magnetic permeability, this is because the oxide samples (4.62 g/cm^3) have a higher density than the slurry sample (3.99 g/cm^3) and therefore have a higher permeability [20].

The magnetic permeability changed with frequency, reaching 1.2 times the initial value as frequency increased for both slurry and press method samples. The forming method (slurry vs. press) did not significantly affect the change in magnetic permeability. Electric permittivity is likely influenced by the density and porosity of the samples, similar to magnetic properties.

The sintering atmosphere and forming method, which affected the sample's microstructure, would likely also impact electric permittivity. The study shows magnetic permeability increasing with frequency. Electric permittivity often decreases with increasing frequency in many materials. Magnetic permeability in ferrites is highly sensitive to crystal structure and composition, as evidenced by the effects of sintering atmosphere. Electric permittivity is generally less sensitive to these factors in ferrites. Magnetic permeability values are typically much larger than electric permittivity values, reflecting their strong magnetic properties.

3.7. Microstructural study

Figs. 8 and 9 examine the microstructural studies of samples sintered under different furnace atmospheric conditions (oxide-hydrogen-nitrogen). According to Fig. 8, the ferrite grains do not have smooth edges, which could be due to the absence of the gamma phase in the oxide samples. The presence of oxygen in the furnace atmosphere can

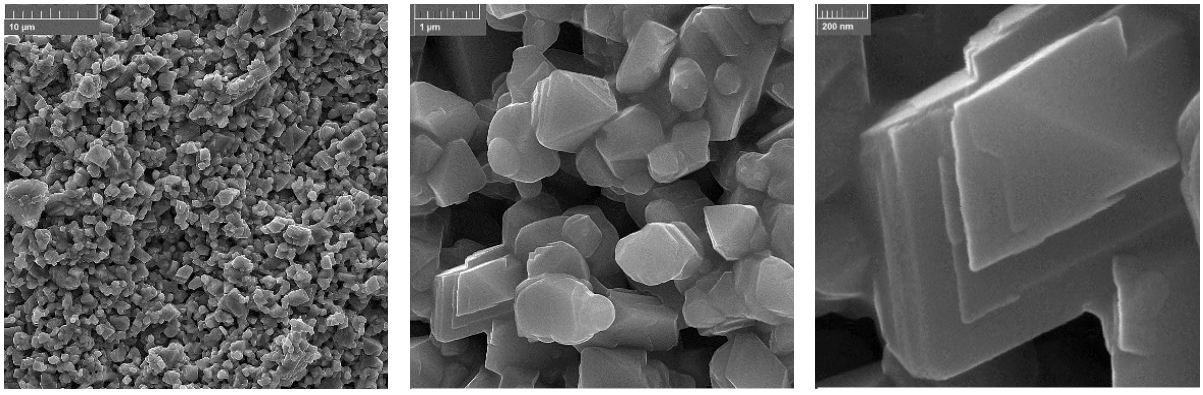

Fig. 10. SEM images of sample 17 sintered and pressed under pure hydrogen atmosphere.

lead to an increase in grain growth in sample 3 in the oxide atmosphere by about 5 μm [2]. According to the results of Fig. 9, the use of nitrogen atmosphere in sample 13 leads to a grain growth of about 2 μm and is controlled in the $ZnMnFe_2O_4$ composition compared to other oxide and hydrogen sintering atmospheres. Therefore, a nitrogen atmosphere is useful for promoting uniform grain growth of $ZnMnFe_2O_4$. It has been proven that in a nitrogen atmosphere, due to the stability of the austenite phase with nitrogen diffusion, condensation is not complete, and the transformation of austenite to gamma ferrite does not occur completely [20].

The grain size in hydrogen atmosphere in sample 14 at 1050 °C was significantly smaller compared to other sintering atmospheres (Fig. 10). It has been said that long sintering time and high heating rate increase the density of samples in hydrogen atmosphere, or in other words, for better densification in hydrogen atmosphere, a long time is required for grain growth, which since the retention time for the samples under study did not change, it can be said that the present finding can be in accordance with the findings of others [19]. On the other hand, it seems that the number of grains with smooth edges, which refers to the gamma phase, is higher in this sintering atmosphere than in oxide samples [20]. It has been said that the presence of the gamma phase can be effective in reducing the real permittivity and increasing the virtual magnetic permittivity [21].

4. Conclusions

The composition of the samples was prepared with a molar ratio of Fe_2O_3-0.5ZnO-0.5Mn_3O_4. Two forming methods: dry pressing at a pressure of 50 MPa and slurry pressing with 10% by weight of water. The samples were sintered at a temperature of 1050 °C and in three atmospheres: oxidizing (normal air), neutral (argon), and reducing (hydrogen and argon). Density, porosity, and shrinkage were measured by the ASTM C373-88 method; microstructural tests were performed by SEM, and phase tests by XRD; magnetic properties were measured by an RF analyzer in the frequency range of 10^7–10^9 Hz. The highest density was for argon dry pressing (4.88 g/cm³), and the lowest porosity was for argon slurry pressing (1%) and hydrogen dry pressing (1%). The samples were reported to be between 15 and 22% in most methods, but slightly higher shrinkage and sometimes higher porosity were observed in slurry samples. The grain size of the samples decreased in argon and nitrogen environments and reached 1 to 2 μm (compared to five microns in the oxidant). Magnetic and electrical properties, the magnetic permeability of the samples reached 1.2 times the initial value with increasing frequency, and no significant difference was observed between the two dry pressing and slurry pressing methods. The samples sintered in argon had about two percent less porosity than in the oxidant, and a more uniform $ZnMnFe_2O_4$ phase was formed. Sintering in nitrogen and hydrogen environments caused the production of the gamma phase and a reduction in grain size, which has a positive effect on the uniformity of the structure. The explicit and unbiased conclusion is that using slurry pressing with argon is the best method to reduce porosity and produce small parts with a uniform structure. The final porosity in this method was only 1%, the density was about 4.7–4.9 g/cm³, and the grain size was reduced to 1–2 μm. The samples sintered in a neutral atmosphere (argon) had about 2% less porosity and a more uniform spinel phase compared to the oxidizing one; the shrinkage results in both methods varied between 18 and 22%. In hydrogen, the grain size was smaller, and the probability of the gamma phase was higher; a certain improvement in the magnetic properties of the samples occurred, but a two-phase structure and different colors were observed. There was no difference between the dry pressing method and the slurry pressing method in terms of the change in magnetic permeability with increasing frequency, and both showed a value of 1.2 times the initial value. This property was enhanced by reducing porosity. Cracking, delamination, and two-phase formation were observed in some dry-pressed samples with high adhesive or porosity, which is not recommended for industrial production. Final conclusion: The use of slurry pressing and sintering in argon is recommended for the production of small, high-density parts with minimal porosity. Control of the atmosphere and pressing pressure plays a key role in reducing grain size, phase uniformity, and increasing magnetic permeability. The numerical results of this paper are fully reliable and acceptable and are a guide for the industrial production of MnZn ferrites.

CRediT authorship contribution statement

Aida Faeghinia: Conceptualization, Methodology, Formal Analysis, Data curation, Investigation, Writing – original draft, Visualization, Writing – review & editing, Project administration, Supervision.

Data availability

The data underlying this article will be shared on reasonable request to the corresponding author.

Declaration of competing interest

The author declares no competing interests.

Funding and acknowledgment

The author gratefully acknowledges the generous support provided by the Materials and Energy Research Center.

References

[1] S. Bid, S.K. Pradhan, Preparation of zinc ferrite by high-energy ball-milling and microstructure characterization by Rietveld's analysis, Mater. Chem. Phys. 82 (2003) 27–37. https://doi.org/10.1016/S0254-0584(03)00169-X.

[2] K. Masters, Spray drying handbook, George Godwin Ltd., London. (1985).

[3] J.T. Fell, J.M. Newton, Determination of tablet strength by the diametral-Compression test, J. Pharmacol. Sci. 59 (1970) 688–691. https://doi.org/ 10.1002/jps.2600590523.

[4] A.S. James, W.M. Dawson, T.J. Daviese, Compaction and Green Strength of Ferrite Powders, Powder Metall. 30 (1987) 267. https://doi.org/10.1179/pom.1987.30.4.267.

[5] N. Özkan, B.J. Briscoe, Characterization of die-pressed green compacts J. Eur. Ceram. Soc. 17 (1997) 697–711. https://doi.org/10.1016/S0955-2219(96)00090-8.

[6] R.C. Kambale, P.A. Shaikh, S.S. Kamble, Y.D. Koleka, Effect of cobalt substitution on structural, magnetic and electric properties of nickel ferrite. J. Alloys Compd. 478 (2009) 599–603. https://doi.org/10.1016/j.jallcom.2008.11.101.

[7] A.A. Hossain, S.T. Mahmud, M. Seki, T. Kawai, H. Tabata, Structural, electrical transport, and magnetic properties of Ni1−xZn xFe2O4. J. Magn. Magn. Mater. 312 (2007) 210–219. https://doi.org/10.1016/j.jmmm.2006.09.030.

[8] H. J. Glass, G. de With, M.J.M. de Graaf, R. J. A. van der Drift, Compaction of homogeneous (Mn, Zn)-ferrite potcores, J. Mater. Sci. 30 (1995) 3162–3170. https://doi.org/10.1007/BF01209232.
[9] J.M Heintz, F Weill, J.C Bernier, Characterization of agglomerates by ceramic powder compaction, Mater. Sci. Eng: A. 109, (1989) 271–277. https://doi.org/10.1016/0921-5093(89)90599-6.
[10] R.L.K. Matsumoto, Generation of Powder Compaction Response Diagrams, J. Amer. Ceram. Soc. 69 (1986) C-246– C-246. https://doi.org/10.1111/j.1151-2916.1986.tb07351.x.
[11] K.G. Webber, O. Clemens, V. Buscaglia, B. Malič, R.K. Bordia, et al., Review of the opportunities and limitations for powder-based high-throughput solid-state processing of advanced functional ceramics, J. European Ceramic Society, 44 (2024) 116780. https://doi.org/10.1016/j.jeurceramsoc.2024.116780.
[12] G. Kogias, Improvement of the properties of MnZn ferrite power cores through improvements on the microstructure of the compacts, J. Magn. Magn. Mater. 324 (2012) 235–241. https://doi.org/10.1016/j.jmmm.2011.07.055.
[13] P. Thakur, D. Chahar, S. Taneja, N. Bhalla, A. Thakur, A review on MnZn ferrites: Synthesis, characterization and applications, Ceram. Int. 46 (2020) 15740–15763. https://doi.org/10.1016/j.ceramint.2020.03.287.
[14] D.T. Gethin, N. Solimanjad, P. Doremus, D. Korachkin, Friction and its Measurement in Powder Compaction Processes, Modelling of Powder Die Compaction, Springer, London. (2008) 105–129. https://doi.org/10.1007/978-1-84628-099-3_8.
[15] H.J. Glass, Compaction Behavior of (MnZn)-Ferrite Granulate, Ph.D Thesis, Eindhoven University of Technology, the Netherlands, (1994). https://doi.org/10.6100/IR415055.
[16] M. Mirshekari, A. Ghasemi, B. Shokrollahi, Glycine-nitrate auto-combustion synthesis and magnetic properties of Mn-Zn ferrites, J. Magn. Magn. Mater. 650 (2024) 43–53. https://doi.org/10.1016/j.jmmm.2023.167089.
[17] A.K. Singh, S.K. Sharma, P.K. Sahoo, R.N. Basu, Preparation and magnetic properties of MnZn ferrite powder compacts by pressing and sintering, J. Magn. Magn. Mater. 536 (2024) 168193. https://doi.org/10.1016/j.jmmm.2024.168193.
[18] G. Rana, P. Dhiman, A. Kumar, D.-V.N. Vo, G. Sharma, et al., Recent advances on nickel nano-ferrite: A review on processing techniques, properties and diverse applications, Chem. Eng. Res. Des. 175 (2021) 182–208 https://doi.org/10.1016/j.cherd.2021.08.040.
[19] US20050098760A1Process for producing granules for being molded into ferrite, granules for being molded into ferrite, green body and sintered body US20050098760A1.
[20] H.J. Glass, G. de With, M.J.M. de Graaf, R.J.A. van der Drift, Compaction of homogeneous (Mn, Zn)-ferrite potcores, J. Mater. Sci. 30 (1995) 3162–3170. https://doi.org/10.1007/BF01209232.
[21] A. Rafferty, T. Prescott, D. Brabazon, Sintering behaviour of cobalt ferrite ceramic. Ceram. Int. 34 (2008) 15–21. https://doi.org/10.1016/j.ceramint.2006.07.012.